Light driven microflow in ice

Franz M. Weinert, Max Wühr, and Dieter Braun[a)]

Department of Physics, Systems Biophysics, Center for Nanoscience, Ludwig Maximilians Universität München, Amalienstr. 54, 80799 München, Germany

We optically pump water through micrometer thin ice sheets. The ice is locally moved with speeds exceeding 5 cm/s by repetitive melting and freezing, which occurs around a moving infrared laser spot. The minimal channel width is 10 μm. The diffusion limitation of ice allows for fast spatial biomolecule control without predefined channels, valves, or external pumps. Dye molecules are pumped across an ice-ice interface, showing the possibility of microfluidic applications. Pumping in ice is three orders of magnitude faster than the previously shown for thermoviscous pumping in water. © *2009 American Institute of Physics.* [DOI: 10.1063/1.3097206]

The ability to remotely control matter with light has unique advantages. Optical tweezers for example can remotely move microscale objects[1] and have allowed many applications in the life science.[2] Likewise, photolithography allows patterning of materials without physical contact at an ever increasing level of miniaturization.[3] A method, which can manipulate not only solids but also fluids by light is equally desirable. In the past, we have pursued nonlinear effects in thermal expansion to optothermally pump fluids.[4,5] Here we applied a similar principle to ice and found that the melting transition dynamics enhance the pump speed significantly i.e., from 50 μm/s to 5 cm/s.

Classical microfluidics provides the highly complex manipulation of small volumes[6–10] in life sciences by pumping fluids through defined channel networks.[11–15] However, a considerably complex external interfacing of the microchannels with pumps and inlets is required. Recently a method to create reconfigurable microchannels in ice by using an IR laser was shown.[16] Our work extends the approach by showing that a moving laser spot in ice yields high pump velocities and has the potential to complement channel-based microfluidics in optically driven platforms.

We create a moving spot of raised temperature by scanning a focused infrared laser through a micrometer thin ice sheet [Fig. 1(a)]. The ice melts at the laser spot and freezes again behind it. The result is a fluid flow in the molten ice in the direction of the moving spot. Since the thermal relaxation time is below milliseconds in microscale fluid or ice films, the laser spot movement can be repeated near the kilohertz regime. As a result, pump velocities of 50 mm/s can be reached along freely defined patterns at the micrometer scale. As an example, Fig. 1(b) demonstrates fluid flow along the pattern "nim."

A chamber with a 3 μm thin fluid layer is sandwiched between a bottom, double-polished silicon wafer, which is cooled by a microscope stage below 0 °C and a top glass window [Fig. 1(c)]. Imaging with a fluorescence microscope (Axiotech Vario, Zeiss) is provided from the top by a charge coupled device camera (Luca S DL-658M, Andor) and a 20× objective (UPlanSApo NA=0.75, Olympus), illuminated with either a xenon lamp (HXP 120, Zeiss) or a light-emitting diode (LED) (LXHL-LD3C, Luxeon). The wave-

length of the heating laser (TLR-10–1940, IPG Photonics) is 1940 nm where water absorbs with an attenuation length of a_{water}=74 μm and ice with a_{ice}=7 μm. The total absorbed power ranged between 0.04–0.08 W for water and 0.7–1.3 W for ice. The laser beam is scanned from below the chamber with a galvanometer mirror pair (6200-XY, Cambridge Technology) and focused with a lens (f=15 mm, LA1540-C, Thorlabs) through the silicon slide, which is transparent for the used wavelength.

Consider a spot of enhanced temperature moving through a thin ice sheet [Fig. 1(a)]. The ice thaws at the front of the spot and freezes in its wake. The density change during the phase transition induces divergent flows due to mass conservation,[17] with a sink (div $\boldsymbol{v}<0$) at the front and a source (div $\boldsymbol{v}<0$) at the back. The solid ice boundaries confine the liquid flow such that movement is from the back of the molten spot to its front. We assume a parabolic flow
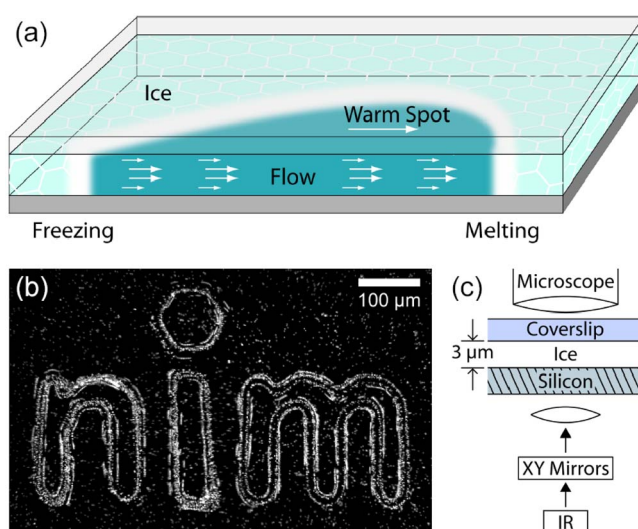

FIG. 1. (Color online) (a) An optically created temperature spot is moved to the right in a sheet of ice. The ice melts in front of the spot (right) and freezes behind it (left) and moves the fluid due to the difference in specific volume. (b) Pumping ice is possible along freely defined patterns such as the letters "nim." The heating laser spot traces the letters nim at 10 Hz. The temporarily molten channels are 25 μm wide and 3 μm thick. We visualize the flow by overlaying differences of successive pictures of fluorescent 1 μm polystyrene spheres, which are suspended in the ice. (c) The laser spot is focused from below and moved with galvanometric mirrors.

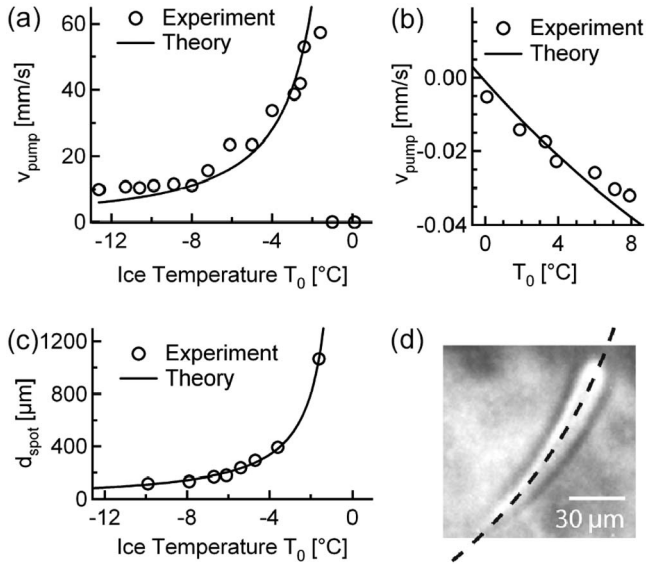[a)]Electronic addresses: braun@lmu.de and dieter.braun@physik.lmu.de.

FIG. 2. (a) Pump velocities depend on the ice temperature T_0 (open circles). The theory of Eq. (3) predicts the pump velocity. (b) When the fluid does not freeze along the channel, the residual negative pump velocities can be described by the theory of thermoviscous flow (Ref. 5). (c) The length of the thawed spot becomes more elongated for higher T_0. (d) Stroboscopic image of the molten spot along a circular path, shown by the broken line.
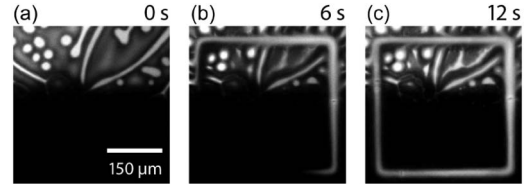

FIG. 3. Optically pumping across an ice-ice interface. [(a)–(c)] The fluorescent dye Cy5 was pumped across an ice-ice interface. The ice-ice interface was created by sandwiching 0.6 μl distilled water to a thickness of 5 μm. After cooling to −12 °C a droplet of 180 μM Cy5 in 1×SSC (150 mM NaCl in 15 mM sodium citrate) is pipetted at the chamber edge and pulled inside by capillary forces. The Cy5 solution freezes after making contact with the ice sheet and forms an interface with the frozen water. The inhomogeneous structure results from the freezing of the dye solution on a slow time scale.

profile perpendicular to the glass/silicon boundaries with $v_{avg} = 2/3 v_{water}$, where v_{water} is the peak velocity in the center of the fluid sheet. The continuity equation $\dot{\rho} + \text{div } \mathbf{j} = 0$ at the water-ice boundary is given by

$$\frac{\rho_{water} - \rho_{ice}}{\Delta t_M} - \frac{2}{3} \frac{v_{water} \rho_{water}}{\Delta x_M} = 0. \tag{1}$$

With the velocity of the water-ice boundary $v_{spot} = \Delta x_M / \Delta t_M$ we find

$$v_{water} = \frac{3}{2} \frac{\rho_{water} - \rho_{ice}}{\rho_{water}} v_{spot}. \tag{2}$$

The water is molten during the passage of the spot for the time interval $\Delta t = d_{spot} / v_{spot}$, where d_{spot} is the end to end distance of the molten area and moves by the distance $\Delta x = v_{water} \Delta t$. If the spot movement is repeated with frequency f, we expect a pump velocity

$$v_{pump} = \Delta x f = \frac{3}{2} \frac{\rho_{water} - \rho_{ice}}{\rho_{water}} d_{spot} f. \tag{3}$$

It is possible to image the length of the moving spot d_{spot} by stroboscopic white light imaging. The on times of the LED of 20 μs are considerably faster than the typical spot passage time $\tau = d_{spot} / v_{spot} = 0.8$ ms. A typical image of the drop-shaped molten area with $d_{spot} = 120$ μm is shown in Fig. 2(d). Pumping is performed with a repetition rate of $f = 650$ Hz and a chamber temperature of $T_0 = -9.9$ °C. With densities $\rho_{water} = 1000$ kg/m^3 and $\rho_{ice} = 917$ kg/m^3 we expect $v_{pump} = 9.5$ mm/s. Experimentally, we find 11 mm/s, which is inferred from tracer particles with 1 μm diameter, in agreement with the theoretical expectations.

The length of the molten spot depends on the temperature of the ice sheet [Fig. 2(c)]. At low ice temperatures, only a short spot is molten. At higher ice temperatures, the molten spot can reach lengths beyond 500 μm/s with the pump velocity exceeding 50 mm/s [Fig. 2(a)]. We fit the spot

length phenomenologically with $d_{spot} = a_0 (a_1 - T)^{a_2}$ and inserted this result into Eq. (3), shown as a solid line in Fig. 2(a). Theory and experiment match quantitatively.

For further increased chamber temperatures, the front of the thawed spot catches up with the back of the previous heating cycle. The fluid flow is not confined solely toward the front in this case and pumping stalls. A residual negative pump velocity is attributed to thermoviscous flow in liquids[4,5] and matches theoretical predictions with a temperature spot width of $b = 60$ μm and a temperature raise of $\Delta T = 15$ K given by

$$v_{pump}^{(fluid)} = -\frac{3\sqrt{\pi}}{4} f \alpha \beta b \Delta T^2, \tag{4}$$

using the thermal expansion coefficient α and temperature dependent viscosity β of water [Fig. 2(b)].[5]

To demonstrate microfluidic applications, we placed two frozen solution next to one another [Fig. 3(a)]. The ice at the top contains the dye Cy5 ($M_W \approx 500$ g/mol) and shows an inhomogeneous structure, probably due to grain boundaries of the slow freezing process. We pump the dye across the ice-ice interface along a rectangular pattern with repetition frequency of 50 Hz [Figs. 3(a)–3(c); $t = 0, 6, 12$ s]. A thin air film is likely to exist between the ice-ice interface and reduces the pump velocity (see movie, supplementary material).[18] The Cy5 dye is pumped along 15 μm wide channels in the bottom ice sheet. The fast freezing process, which is on the millisecond timescale, yields homogeneous Cy5 concentrations along the channel.

The pump paths can be defined within optical resolution and can be changed dynamically within tens of milliseconds. This can be used to implement switches and valves. Ice allows the deposition of substances at any place without loosing the specimen by diffusion, while speeds are in the centimeter per second range even for small temperature steps across the melting point. We expect that the repetitive melting-freezing cycles are not very stressful to biomolecules since ice, if cooled on the millisecond time scale, remains amorphous and without gain boundaries.

The creation of vapor bubbles imposes restrictions on the pump mechanism. The density shift in the initial thawing can reduce the pressure in the chamber below the triple point of water ($p_{triple} \approx 6$ mbar) and introduce water vapor bubbles, which typically do not dissolve back into the water or ice and hinder pumping. To reduce their generation, elastic chamber boundaries could be used.

To conclude, we expanded the thermoviscuous paradigm of light driven microfluidics by switching from fluid to ice sheets. In ice the pump speed was in the cm/s regime without excessive heating. The fluid flow was quantitatively explained by a model of directed fluid flow inside a moving thawed area. Laser heating in ice allows for highly flexible fluid flow along optically definable patterns without lateral diffusion of dissolved molecules. We demonstrated the exchange of picoliter volumes across an ice-ice interface. With the results, we envisage complex light driven microfluidics in ice.

[1] A. Ashkin, Phys. Rev. Lett. **24**, 156 (1970).

[2] D. M. Block, L. S. B. Goldstein, and B. J. Schnapp, Nature (London) **348**, 348 (1990).

[3] P. S. Peercy, Nature (London) **406**, 1023 (2000).

[4] F. M. Weinert, J. A. Kraus, T. Franosch, and D. Braun, Phys. Rev. Lett. **100**, 164501 (2008).

[5] F. M. Weinert and D. Braun, J. Appl. Phys. **104**, 104701 (2008).

[6] R. B. M. Schasfoort, S. Schlautmann, J. Hendrikse, and A. van den Berg, Science **286**, 942 (1999).

[7] J. Tian, H. Gong, N. Sheng, X. Zhou, E. Gulari, X. Gao, and G. Church, Nature (London) **432**, 1050 (2004).

[8] M. A. Burns, B. N. Johnson, S. N. Brahmasandra, K. Handique, J. R. Webster, M. Krishnan, T. S. Sammarco, P. M. Man, D. Jones, D. Heldsinger, C. H. Mastrangelo, and D. T. Burke, Science **282**, 484 (1998).

[9] J. W. Hong, V. Studer, G. Hang, W. French Anderson, and S. R. Quake, Nat. Biotechnol. **22**, 435 (2004).

[10] T. Thorsen, S. J. Maerkl, and S. R. Quake, Science **298**, 580 (2002).

[11] A. Manz, N. Graber, and H. M. Widmer, Sens. Actuators B **1**, 244 (1990).

[12] D. J. Harrison, K. Fluri, K. Seiler, Z. Fan, C. S. Effenhauser, and A. Manz, Science **261**, 895 (1993).

[13] S. C. Jacobson, R. Hergenroder, L. B. Koutny, and J. M. Ramsey, Anal. Chem. **66**, 1114 (1994).

[14] A. T. Woolley and R. A. Mathies, Proc. Natl. Acad. Sci. U.S.A. **91**, 11348 (1994).

[15] T. M. Squires and S. R. Quake, Rev. Mod. Phys. **77**, 977 (2005).

[16] M. Varejka, S. Piletsky, A. Woodman, A. P. F. Turner, 2006 Digest of the LEOS Summer Topical Meetings, 36 (2006).

[17] E. Yariv and H. Brenner, Phys. Fluids **16**, L95 (2004).

[18] See EPAPS Document No. E-APPLAB-94-112910 for a supplementary movie. For more information on EPAPS, see http://www.aip.org/pubservs/epaps.html.